J. Opt. A: Pure Appl. Opt. **10** (2008) 055202 (6pp) doi:10.1088/1464-4258/10/5/055202

Modulation of the gold particle–plasmon resonance by the metal–semiconductor transition of vanadium dioxide

J Y Suh[1], E U Donev[1], D W Ferrara[1], K A Tetz[1], L C Feldman[1,2] and R F Haglund Jr[1]

[1] Department of Physics and Astronomy, Vanderbilt Institute of Nanoscale Science and Engineering, Vanderbilt University, Nashville, TN 37235, USA
[2] Department of Physics and Astronomy, Rutgers, The State University of New Jersey, Piscataway, NJ 08854, USA

E-mail: eugene.donev@vanderbilt.edu

Received 15 January 2008, accepted for publication 11 March 2008
Published 31 March 2008
Online at stacks.iop.org/JOptA/10/055202

Abstract
We report experimental observations of relative blue-shifts in the particle–plasmon resonance of gold nanoparticles (Au NPs) covered with a vanadium dioxide (VO_2) film as the VO_2 material undergoes a semiconductor-to-metal transition at approximately 67 °C. Although the extinction spectra of the Au NPs exhibit significant red-shifts in the presence of the surrounding VO_2 film as compared to the same particles in air, the key result of this work is the dynamically controlled blue-shift of the Au-NP dipole resonance upon thermal switching of the VO_2 overlayer from the semiconducting to the metallic state. We also report on the size and polarization dependence of the extinction spectra for both states, and present Mie theory calculations that confirm in a semi-quantitative way the observed trends in the VO_2-induced modulation of the Au-NP plasmon resonance, and their origin in the VO_2 dielectric function.

Keywords: localized surface-plasmon resonance, LSPR, extinction blue-shift, metal–semiconductor transition, vanadium dioxide, VO_2, gold, Au, nanoparticles, pulsed-laser deposition, PLD, nanocomposite

(Some figures in this article are in colour only in the electronic version)

1. Introduction

Metal nanoparticles (NPs) exhibit characteristic absorption and scattering bands in the visible range due to the electromagnetic interaction of light with oscillating surface charges, the so-called localized surface-plasmon resonance (LSPR) or simply the particle–plasmon [1]. The LSPR is distinct from the propagating surface-plasmon polariton (SPP) in that the excited LSPR mode is spatially confined within the particles. As pointed out by Cortie *et al* [2], an important current issue in plasmonics is the possibility of 'self-regulating' the LSPR of composite metallic NPs: for instance, under a sufficiently intense light irradiation, the dynamic functionality of such NPs could be used as a probe in photothermal therapy or optical sensing applications [3, 4].

Vanadium dioxide:gold (VO_2:Au) composite material is a practical candidate for enabling such spectral modulation, as has been shown in the case of extraordinary optical transmission through subwavelength hole arrays [5, 6]. VO_2 is a transition metal oxide that exhibits a semiconductor-to-metal phase transition as the temperature is raised above the critical temperature ($T_c \approx 340$ K), which is accompanied by changes in the crystalline structure and a large transmission contrast in the near-infrared range. VO_2 possesses its own plasmonic resonance, albeit heavily damped, around 1.1 μm [7, 8], while Au NPs are known to have relatively strong extinction (scattering + absorption) cross-sections at visible or near-infrared wavelengths [9].

There are two recent experimental studies on metal NPs in a VO_2 matrix. In one case [10], Xu *et al* sputtered

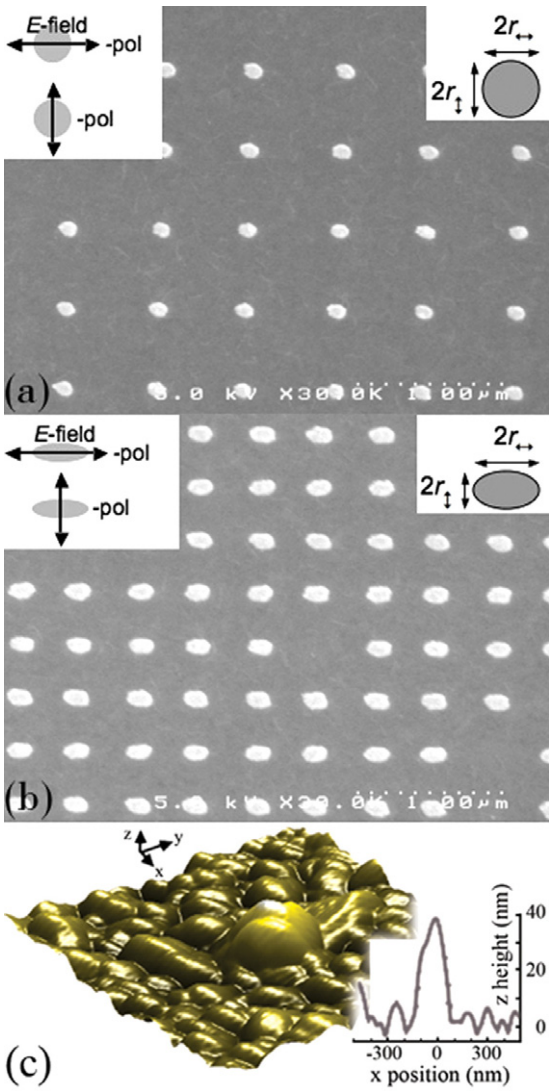

Figure 1. SEMs of (a) circular and (b) elliptical Au NPs. (c) AFM and (inset) line scan of a single Au NP covered with crystalline grains of a VO_2 film. The schematic insets in (a) and (b) show the conventions used throughout the text for the incident-light polarization (left) and the geometric parameters of the Au NPs (right).

silver (Ag) on top of a VO_2 thin film; the resulting Ag NPs had a rather broad size distribution of particle diameters ($|\Delta(2r)| = 15$–55 nm), which generally manifests itself as a broadening of the LSPR peaks [11]. Such inhomogeneous broadening of the resonance peak was also observed by Maaza *et al* [12] for a VO_2:Au nanocomposite, made by pulsed-laser deposition (PLD); this effect is most likely due to the small size and broad size distribution of the embedded Au NPs. Moreover, closely spaced NPs—typically found in self-assembled or PLD nanoparticle films—can give rise to particle–particle interactions, and thus cause significant peak shifts [13] in addition to those due to the change in the dielectric environment.

In this report, we systematically explore the modulation of the LSPR on lithographically fabricated Au nanoparticle arrays by means of the reversible metal–semiconductor transition of VO_2. In particular, we exhibit the dependence of this modulation on nanoparticle size, shape, and light polarization. The Au LSPR peaks blue-shift in the metallic state of VO_2 ($T > T_c$) with respect to the semiconducting state ($T < T_c$) by as much as 80 nm for symmetric and 200 nm for asymmetric Au NPs (including polarization effects for the latter). The relative blue-shift is qualitatively predicted by a Mie calculation, modified to take into account the imaginary part of the complex refractive index of the VO_2 medium. For the asymmetric Au NPs, we observe a strong dependence of the plasmon resonance on polarization of the incident light with respect to the particles' major (long) and minor (short) axes, complemented by subtler peak shifts with varying aspect ratios at a fixed polarization.

2. Experimental methods

Using focused-ion-beam (FIB: 30 keV Ga^+) lithography [14] in a poly(methyl methacrylate) (PMMA: ∼50 nm thick) mask, followed by thermal evaporation of Au (∼15 nm thick) and standard lift-off, we patterned arrays of Au NPs of various sizes and shapes, ranging from elliptical cylinders (3:1 aspect ratio in the plane parallel to the substrate) to circular cylinders. In order to minimize over-exposure of the PMMA for the larger particles [15], the dwell time was reduced to approximately 30 μs per FIB pixel. The substrate was a glass slide, coated with indium–tin oxide (ITO) to reduce charging during FIB exposure.

Scanning-electron micrographs (SEMs) of typical arrays are shown in figures 1(a) and (b) before deposition of the vanadium oxide overlayer. Pulsed-laser deposition, followed by thermal oxidation, was performed to make a VO_2 layer (∼50 nm thick) atop the Au-NP arrays: first, the beam from a KrF excimer laser ($\lambda = 248$ nm) was focused onto a vanadium target at a fluence of ∼4 J cm^{-2} to deposit a sub-stoichiometric vanadium oxide ($VO_{\sim 1.7}$); the sample was then annealed at 450 °C under 250 mTorr of oxygen gas for 40 min, in order to convert the amorphous film into stoichiometric, crystalline VO_2 [16]. Figure 1(c) shows an atomic-force micrograph (AFM) of one Au NP covered with the annealed VO_2 film; the grainy texture visible around the central particle is due to the formation of microdomains during crystallization of the amorphous $VO_{1.7}$ film into VO_2. The VO_2 phase transition was confirmed by measuring the thermal hysteresis for infrared transmission ($\lambda = 1330$ nm). The sample was heated and cooled during the transmission measurement using a thermoelectric heat pump, which was mounted on a translation–rotation stage equipped with a precision thermocouple. Optical transmission spectra of the different Au-NP arrays were acquired using linearly polarized white light at normal incidence to the sample surface. The incident-beam spot and array locations were monitored by dark-field scattering. The transmitted light was fiber-fed to a spectrometer with a cooled charge-coupled-device (CCD) detector, and normalized to transmission through the bare VO_2 film (i.e., no Au NPs). The resulting transmittance spectra were post-processed to extract the Au-NP extinction spectra.

3. Results and discussion

The strong electric field localization near a metal NP ensures that particle size and shape [17–19], interparticle

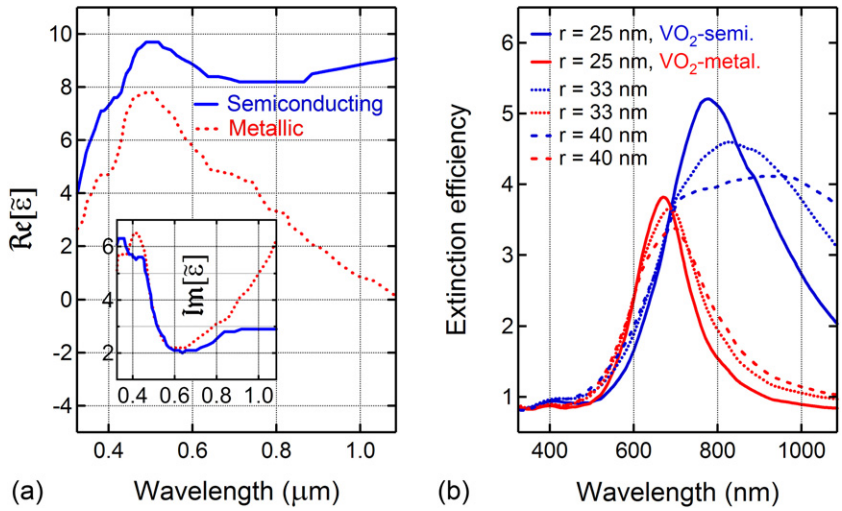

Figure 2. (a) Real and (inset) imaginary parts of the VO_2 permittivities in the visible to near-infrared region (data extracted from [24]). (b) Mie calculations of extinction efficiencies for Au spheres (radius = 25, 33, 40 nm) in VO_2 as a function of wavelength and state of the VO_2 medium.

spacing [13, 20], and dielectric environment [21, 22] all have substantial effects on the extinction spectra. Therefore, the controlled geometrical characteristics of lithographically fabricated NPs offer several distinct ways of modulating the resonant wavelength using the metal–semiconductor transition in an encapsulating thin film of VO_2, some of which are demonstrated below for the VO_2:Au nanocomposite.

The spectral shifts of the particle–plasmon resonance can be understood qualitatively within the framework of the quasi-static approximation for spherical particles. The polarizability (α) of a small ($r \ll \lambda$) metal (Au) sphere immersed in a medium (here, VO_2) can be obtained by solving the Laplace equation [19, 23]; in the simplest case of only dipolar excitations, α incorporates the complex-valued, wavelength-dependent permittivities $\tilde{\varepsilon}(\lambda)$ of the two materials as follows:

$$\alpha(\lambda) = r^3 \frac{\tilde{\varepsilon}_{\mathrm{Au}}(\lambda) - \tilde{\varepsilon}_{\mathrm{VO_2}}(\lambda)}{\tilde{\varepsilon}_{\mathrm{Au}}(\lambda) + 2\tilde{\varepsilon}_{\mathrm{VO_2}}(\lambda)}. \quad (1)$$

The dipole resonance condition for the Au particle requires that the real part of the denominator in equation (1) vanish. Consequently, the LSPR peak occurs in the near-infrared region of the spectrum because there the real part of the Au permittivity becomes negative enough to cancel out its VO_2 counterpart in the oxide's semiconducting state, which maintains values between 8 and 10 at visible to near-infrared wavelengths (figure 2(a)). In the metallic state of VO_2, however, the real part of the permittivity is considerably lower than that in the semiconducting state (figure 2(a)), which entails a less negative Au permittivity for satisfying the dipole resonance condition (equation (1)); hence, the LSPR peak should appear at shorter wavelengths when the surrounding VO_2 has switched into its metallic state. That is, the peak will be blue-shifted with respect to the semiconducting state.

Figure 2(b) shows the extinction efficiencies calculated using Mie theory for spherical Au NPs of different radii embedded in the absorbing VO_2 medium. The permittivities of VO_2 and Au were obtained from [24] and [25], respectively; the effect of temperature on the Au permittivity is negligible [26]. Although the Mie calculations lend rigor to the predictions of the quasi-static approximation for the spectral shifts of the Au LSPR—whether caused by the VO_2 phase transition or by varying particle size—they cannot be compared directly to the experimental peak positions because of the different particle shape (i.e., discs rather than spheres) and the presence of the ITO-coated glass substrate in our experiments. Crucially, however, Mie theory confirms qualitatively the observed blue-shift of the Au particle–plasmon resonance upon switching of the VO_2 matrix from semiconducting to metallic, as evidenced by the experimental spectra below (figures 3 and 4).

Figure 3 shows extinction spectra of arrays of symmetric (i.e., circular) Au NPs of two different radii, approximately 60 nm in (a) and 80 nm in (b), with interparticle spacings of 600 nm. We first note that the Au-NP extinction peaks at room temperature (20 °C) are significantly red-shifted with respect to those taken in the absence of the VO_2 overlayer (not shown). At a high enough temperature (95 °C)—so that the VO_2 layer has already transformed into its metallic state—the spectra move by more than 60 nm towards shorter wavelengths for either polarization direction. Comparing the peak shifts in figures 3(a) and (b), we observe that the LSPRs move further to the blue with decreasing particle size, as confirmed by Mie theory. Since these Au NPs are nearly symmetrical around an axis normal to the surface, the spectra in the two polarization directions are almost identical; slight differences between the two polarizations are likely due to a small, systematic asymmetry in the particle shapes originating from stigmation misalignment of the FIB. This asymmetry is evident in planar-view SEMs (figure 1(a)) showing arrays of nearly circular NPs with a slight skew in a common, arbitrary direction.

The extinction spectra for representative arrays of intentionally asymmetric (i.e., elliptical) Au NPs, covered with a VO_2 layer, are shown in figure 4; the short NP axes ($2r_{\updownarrow}$) are

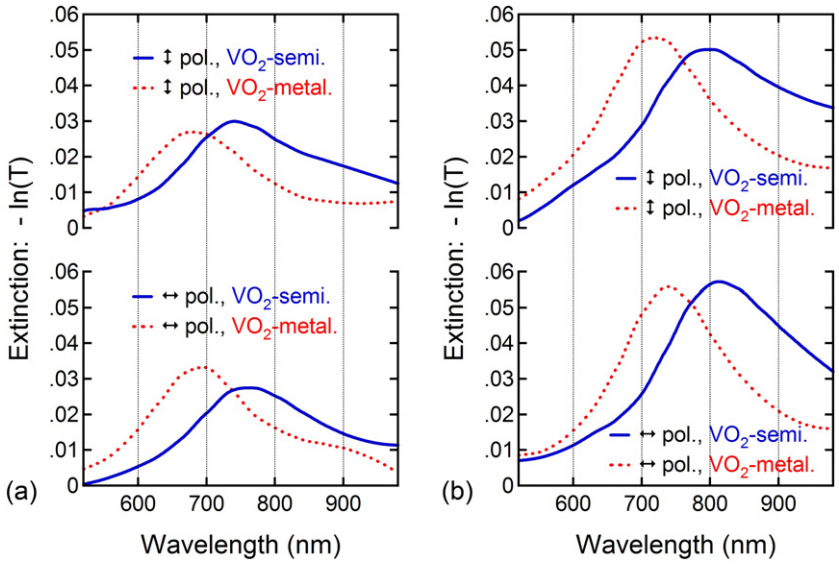

Figure 3. Extinction spectra as a function of wavelength, incident-light polarization, and state of the VO_2 overlayer for arrays of circular (i.e., symmetric) Au NPs of two different diameters ($2r$): (a) 120 nm and (b) 160 nm. Transmittance: T = Intensity{VO_2 + Au NPs + substrate}/Intensity{VO_2 + substrate}.

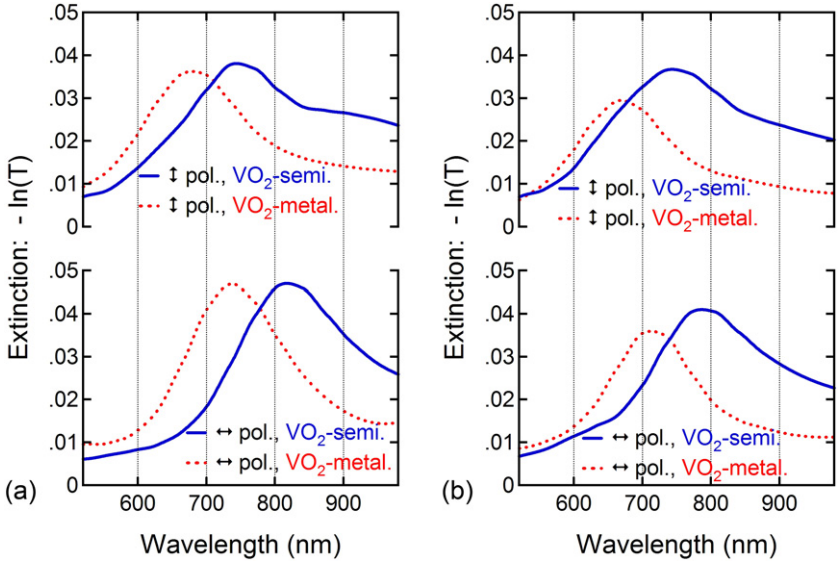

Figure 4. Extinction spectra as a function of wavelength, incident-light polarization, and state of the VO_2 overlayer for arrays of elliptical (i.e., asymmetric) Au NPs of two different aspect ratios ($r_{\leftrightarrow}/r_{\updownarrow}$): (a) 80 nm/60 nm = 1.33 and (b) 70 nm/50 nm = 1.40. Transmittance: T = Intensity{VO_2 + Au NPs + substrate}/Intensity{VO_2 + substrate}.

about (a) 120 nm and (b) 100 nm, while the long axes ($2r_{\leftrightarrow}$) are about (a) 160 nm and (b) 140 nm. Besides LSPR shifts induced by the VO_2 phase transition and similar to those seen for the symmetric NPs, a strong dependence on polarization is also observable in the asymmetric case. When the electric field of the incident light lies parallel to the long axes of the NPs (↔-polarization), the transition-induced blue-shift of the LSPR peaks is more pronounced than when the electric field is parallel to the particles' short axes (↕-polarization). These asymmetric NPs give differences of more than 30 nm in the maximum resonant wavelength for the different polarizations, while there is hardly any shift between the two polarizations for the symmetric NPs. Thus, when compared to the LSPR of a symmetric Au NP of r = 60 nm (figure 3(a)), the resonance peaks of an asymmetric particle of $r_{\leftrightarrow}$ = 70 nm and $r_{\updownarrow}$ = 50 nm (figure 4(b)) exhibit a red-shift for ↔-polarization but a blue-shift for ↕-polarization, in either state of the VO_2 overlayer.

Figure 5(a) summarizes our data on how the LSPR wavelengths (extinction peaks) shift with particle size for the symmetric NPs. The linear fits to the data for the semiconducting and metallic phases of VO_2 yield slightly different slopes. This divergence in resonant wavelengths stems from the permittivity difference between the two phases

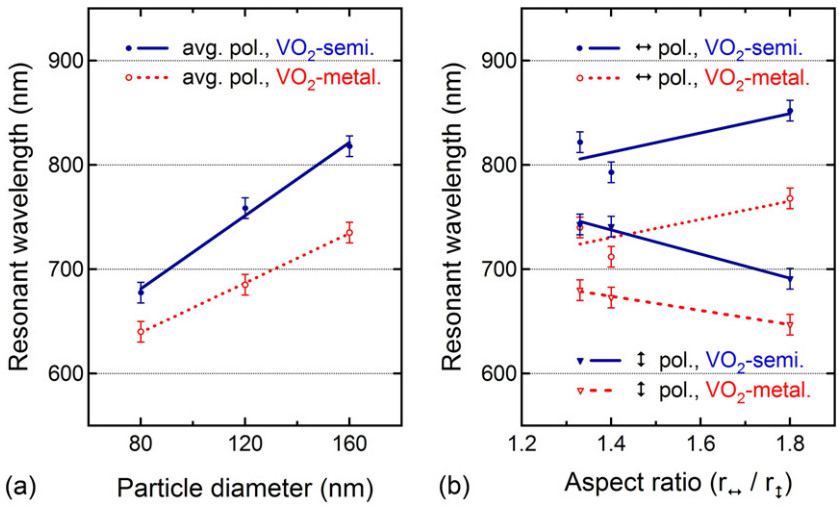

Figure 5. (a) Peak resonant wavelengths, averaged over both incident-light polarizations, as a function of particle size ($2r = 80$, 120, 160 nm) and state of the VO_2 overlayer for the circular (i.e., symmetric) Au NPs. (b) Peak resonant wavelengths as a function of particle aspect ratio ($r_{\leftrightarrow}/r_{\updownarrow} = 80$ nm/60 nm, 70 nm/50 nm, 90 nm/50 nm), incident-light polarization, and VO_2 state for the elliptical (i.e., asymmetric) Au NPs.

of the VO_2 film, which continually increases towards longer wavelengths (figure 2(a)) where larger Au NPs have their resonances. For the largest of our symmetric particles ($2r = 160$ nm), the transition-induced blue-shift of the resonant wavelength is about 80 nm (figure 5(a)). On the other hand, our most asymmetric Au NPs ($r_{\leftrightarrow}/r_{\updownarrow} = 1.80$) can yield blue-shifts as large as 200 nm (figure 5(b)) under the combined effects of the VO_2 semiconductor-to-metal transition and the direction of the incident electric field vector. The red-shift in resonant wavelength with increasing aspect ratio for ↔-polarized light (see the positive-slope lines in figure 5(b)) is brought about by depolarization of the radiation across the particle surface due to the finite ratio of particle size to wavelength, as can be shown by applying electrodynamic corrections to the quasi-static treatment, the so-called modified long-wavelength approximation (MLWA) [19, 27]. Conversely, when the incident electric field oscillates along the short NP axes (↕-polarization), the resonance peaks blue-shift with increasing aspect ratio (see the negative-slope lines in figure 5(b)); the MLWA treatment also reproduces this trend [19, 27].

4. Conclusion

We have demonstrated a method for modulating the spectral features of the localized surface-plasmon resonance of Au nanoparticles by means of the metal–semiconductor transition of VO_2, that is, by dynamically (and reversibly) changing the dielectric properties of the material that covers the Au NPs. The modulation can be thermally controlled, as here, or initiated by a laser pulse on an ultrafast timescale [8].

As predicted by electromagnetic theory, the extinction spectra of the Au NPs exhibit a marked dependence on particle size and shape, incident-light polarization, and, of course, on the state of the VO_2 overlayer, semiconducting or metallic. The spectral shift of the Au LSPR across the VO_2 phase transition is caused by the different dielectric properties of VO_2 in each state: the thermally induced change in the permittivity of VO_2 determines the spectral position of the LSPR wavelength of the VO_2:Au nanocomposite. Invariably, a relative blue-shift of the LSPR peak follows the switching of the VO_2 material from the semiconducting to the metallic state.

We speculate that an improved sample structure, one better suited to quantitative comparisons with Mie theory calculations, would be an array of metal NPs fully embedded in a VO_2 matrix: for example, a 'sandwich' of two 100 nm thick VO_2 films with Au NPs in between. Technically, such a structure would need at least one very flat VO_2 film for successful NP lithography, and that can be grown epitaxially on a transparent substrate like sapphire [28]. Another possible extension of the work presented here may involve laser switching—the use of high-powered laser pulses for launching the LSPR of metal NPs and the metal–semiconductor transition of VO_2 simultaneously. In any case, the VO_2 phase transition emerges as a promising mechanism for dynamically controlling the plasmonic behavior of metal nanoparticles.

Acknowledgment

This work was supported by the US Department of Energy, Office of Science (Grant DE-FG02-01ER45916).

References

[1] Kreibig U, Gartz M, Hilger A and Hovel H 1998 *Optical Investigations of Surfaces and Interfaces of Metal Clusters* vol 4, ed M A Duncan (Stanford: JAI Press)
[2] Cortie M B, Dowd A, Harris N and Ford M J 2007 *Phys. Rev.* B **75** 113405
[3] Hirsch L R, Stafford R J, Bankson J A, Sershen S R, Rivera B, Price R E, Hazle J D, Halas N J and West J L 2003 *Proc. Natl Acad. Sci. USA* **100** 13549–54
[4] Brockman J M, Nelson B P and Corn R M 2000 *Annu. Rev. Phys. Chem.* **51** 41–63
[5] Donev E U, Suh J Y, Villegas F, Lopez R, Haglund R F and Feldman L C 2006 *Phys. Rev.* B **73** 201401

[6] Suh J Y, Donev E U, Lopez R, Feldman L C and Haglund R F 2006 *Appl. Phys. Lett.* **88** 133115
[7] Bianconi A, Stizza S and Bernardini R 1981 *Phys. Rev.* B **24** 4406–11
[8] Rini M, Cavalleri A, Schoenlein R W, Lopez R, Feldman L C, Haglund R F, Boatner L A and Haynes T E 2005 *Opt. Lett.* **30** 558–60
[9] Xia Y N and Halas N J 2005 *MRS Bull.* **30** 338–44
[10] Xu G, Chen Y, Tazawa M and Jin P 2006 *J. Phys. Chem.* B **110** 2051–6
[11] Coronado E A and Schatz G C 2003 *J. Chem. Phys.* **119** 3926–34
[12] Maaza M, Nemraoui O, Sella C, Beye A C and Baruch-Barak B 2005 *Opt. Commun.* **254** 188–95
[13] Rechberger W, Hohenau A, Leitner A, Krenn J R, Lamprecht B and Aussenegg F R 2003 *Opt. Commun.* **220** 137–41
[14] McMahon M D, Lopez R, Haglund R F, Ray E A and Bunton P H 2006 *Phys. Rev.* B **73** 041401
[15] Wang S, Pile D F P, Sun C and Zhang X 2007 *Nano Lett.* **7** 1076–80
[16] Suh J Y, Lopez R, Feldman L C and Haglund R F 2004 *J. Appl. Phys.* **96** 1209–13
[17] Foss C A, Hornyak G L, Stockert J A and Martin C R 1994 *J. Phys. Chem.* **98** 2963–71
[18] Grand J, Adam P M, Grimault A S, Vial A, De la Chapelle M L, Bijeon J L, Kostcheev S and Royer P 2006 *Plasmonics* **1** 135–40
[19] Kelly K L, Coronado E, Zhao L L and Schatz G C 2003 *J. Phys. Chem.* B **107** 668–77
[20] Su K H, Wei Q H, Zhang X, Mock J J, Smith D R and Schultz S 2003 *Nano Lett.* **3** 1087–90
[21] Jensen T R, Duval M L, Kelly K L, Lazarides A A, Schatz G C and Van Duyne R P 1999 *J. Phys. Chem.* B **103** 9846–53
[22] Mock J J, Smith D R and Schultz S 2003 *Nano Lett.* **3** 485–91
[23] Zeman E J and Schatz G C 1987 *J. Phys. Chem.* **91** 634–43
[24] Verleur H W, Barker A S and Berglund C N 1968 *Phys. Rev.* **172** 788–98
[25] Johnson P B and Christy R W 1972 *Phys. Rev.* B **6** 4370–9
[26] Link S and El-Sayed M A 1999 *J. Phys. Chem.* B **103** 4212–7
[27] Sandrock M L and Foss C A 1999 *J. Phys. Chem.* B **103** 11398–406
[28] Jin P, Tazawa M, Yoshimura K, Igarashi K, Tanemura S, Macak K and Helmersson U 2000 *Thin Solid Films* **375** 128–31